7

INJURY BIOMECHANICS RESEARCH
Proceedings of the Thirty-Fourth International Workshop

Material Characterization of the Costal Chondral Junction

A. Lau, M. Kindig, and R. Kent

This paper has not been screened for accuracy nor refereed by any body of scientific peers and should not be referenced in the open literature.

ABSTRACT

Current models of the rib cage contain a discreet junction where the costal cartilage meets the rib bone. However, observations from a previous study find that the junction is not discreet and that this transition region varies in length among different subjects. Further investigation of this junction using a microCT scan found that the bone microstructure around the costal chondral junction extended above and below the cartilage midsubstance through the costal cartilage. The properties of this transition region could affect the frequency and location of rib fractures and be used to improve the current finite element models of the rib cage. This study investigates how the material properties of human ribs vary across costal chondral junction using microCT analysis along with ramp-hold, displacement driven indentation tests performed on the cartilage cross section and outer surface.

INTRODUCTION

Rib fractures are the most common skeletal thoracic injury sustained by restrained occupants in frontal crashes (Pattimore et al., 1992). And studies have found that older drivers are more prone to chest injuries in automotive crashes (Morris et al., 2002). As a result, there has been a recent focus on the study of the rib cage including whole thorax mechanical (Kent et al., 2004), structural characterization of the rib bone (Charpail et al., 2005), and material level characterization of the rib bone through coupon tensile tests (Kemper et al., 2005). However, little work has been done to characterize the costal cartilage, which connects the rib bone to the sternum. The material properties of the costal cartilage could have affects on the mechanical response of the rib cage.

The prevalence of calcification in the costal cartilage increases with increasing age (Rejtarova et al., 2004). In addition, the most severe levels of calcification are more prevalent in the oldest age groups (Teal, et al., 1989). With the increasing number of older drivers, the calcification of the costal chondral junction could alter the effectiveness of the current restraint systems for these occupants. These regions of calcification could alter the mechanical response of the thorax and could lead to a source of stress concentration. This could increase the likelihood of obtaining rib fractures during frontal loading and could also alter the location of these rib fractures.

Finite Element simulations showed that modifying the material properties of the costal cartilage region changed the stress distribution in the rib bone for hub loading (Figure 1).

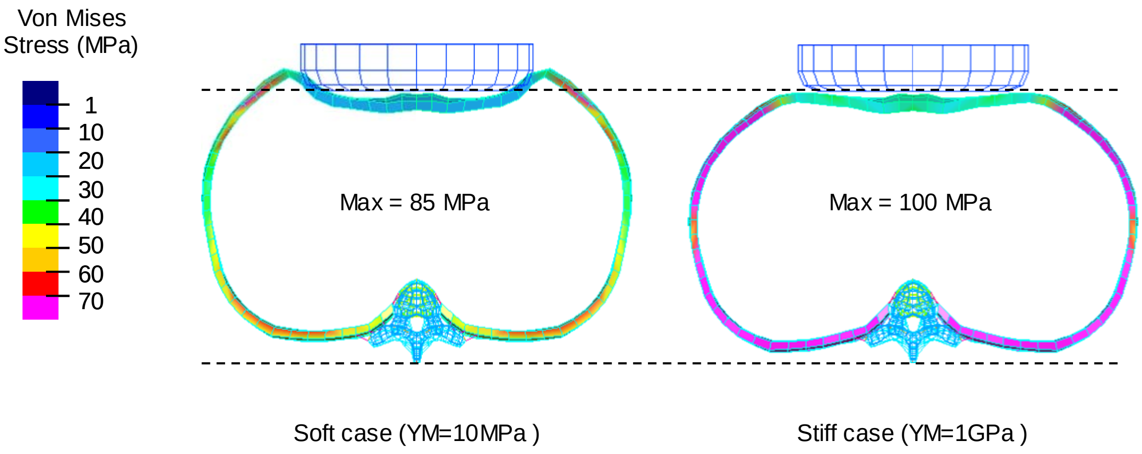

Figure 1: Comparison of the deformed mesh and von Mises stress contours for finite element model of the fifth rib for costal cartilage modulus of 10 MPa (left) or 1 GPa (right).

In addition, the H model of the rib cage contains a discreet junction between the costal cartilage and rib bone (Figure 2). The costal cartilage in this model was given an elastic modulus of 339 MPa (H-model ver. 2.1). Observations in the laboratory reveal that this discreet junction from cartilage to rib bone is not necessarily the case. And previous studies found the instantaneous elastic modulus of the costal cartilage midsubstance to be around 5.2MPa for spherical indentation (Lau et al., 2006) and found the bending modulus for costal cartilage to be around 7.1MPa under 3 point bending (Roy et al., 2004). This study aims to better understand and characterize the transition of the costal cartilage junction and the rib bone through material tests via spherical indentation and microCT analysis.

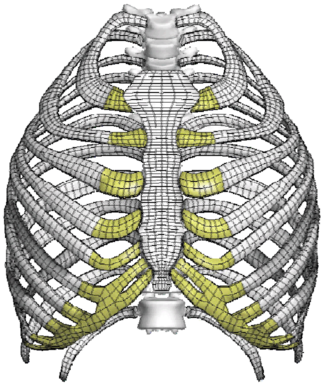

Figure 2: H Model of the Thorax. Costal cartilage elements are yellow.

Indentation testing is common for methods of testing biological materials and is one of the most common methods for test material characterization of articular cartilage (Mow et al., 2005). Unlike traditional tensile tests, indentation testing is considered non-destructive to the sample. During indentation testing, a probe that is relatively small compared to the specimen is brought into contact with the surface and driven into the specimen under a constant load condition or under a prescribed displacement. Then the displacement-time (for load control) or force-time (for displacement control) response can be measured.

Many different tip geometries can be chosen including a flat punch, conical, pyramidal, and (hemi) spherical. Because of its insensitivity to alignment, spherical indentation is useful for testing biological materials, even though the analysis is more complex than for one with a flat punch (Cheng et al., 2005). In this study, ramp-hold, displacement-controlled, spherical indentation was the chosen method for material characterization.

In addition to investigating the local material properties along the costal cartilage and rib, micro computed tomography (microCT) was use to examine the local geometries. MicroCT has been used to analyze the microstructure of trabecular bone (Laib and Ruegsegger, 1999) and also the mineral content of bone (Gupta et al., 2005). This is useful because the geometries and mineral composition of the calcifying costal cartilage and costal chondral junction are still unknown.

The current study looks at the local material properties of the costal cartilage and rib bone by performing surface indentations from the costal cartilage, across the costal chondral junction and into the rib bone. Instantaneous and relaxed modulus values can be obtained from these indentation tests. In addition, the use of microCT scans can help provide highly detailed geometries of the rib specimens.

METHODS

Materials and Specimen Preparation

Polyurethane rubber sheets with a known elastic modulus E = 4 MPa (PS-4 polyurethane, Vishay Measurments) were used as the calibration standard for indentation experimental setup and also used to monitor the consistency of the indentation tests.

Costal cartilage tissue was obtained from young porcine rib cages. The rib segments and costal cartilage were excised from the sternum to about 1.5 - 2 cm distal to the costal chondral junction (CCJ). It was then cleaned of external muscle tissue (Figure 3).

Figure 3: Costal Cartilage and Rib Segment that has been cleaned of the intercostal tissues.

The samples were placed into 30 mm diameter Falcon™ tubes and microCT scans were performed at 30 µm isotropic resolution on a Scanco VivaCT scanner (Scanco Medical, Switzerland) (Figure 4). The three dimensional reconstruction of the microCT data were performed with Voxar 3D (Barco Medical Imaging).

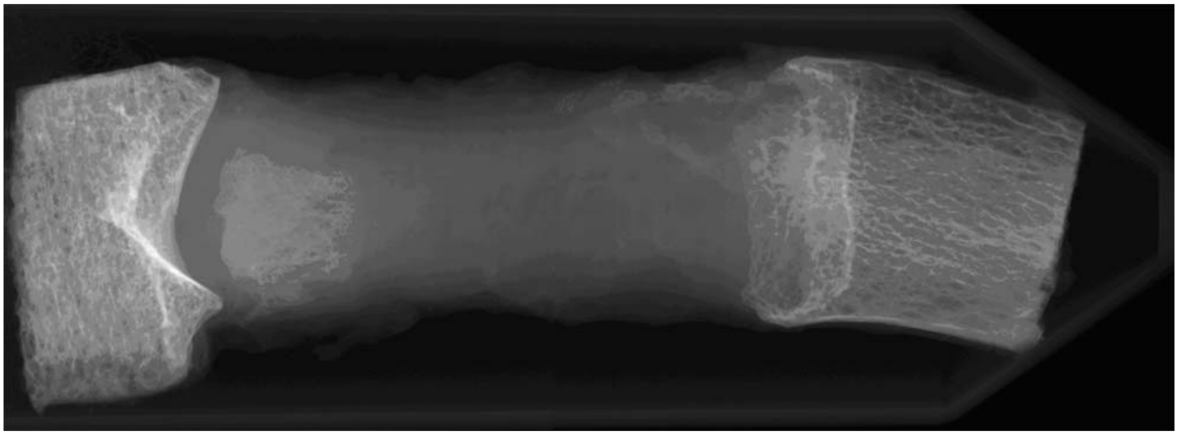

Figure 4: Scout view of a rib specimen inside the microCT scanner. The sternum is on the left and the rib bone on the right.

After scanning, the sternum was removed and the specimen was embedded into R1 FAST CAST™ 891 (Goldenwest Manufacturing Inc.) urethane resin (Figure 5). The fast cast was given at least an hour to completely cure. Then these samples were soaked in physiological saline at least 30 minutes before performing surface indentations. After visual inspection, additional removal of the perichondrial and periostial layer was performed to ensure a clean surface for indentation.

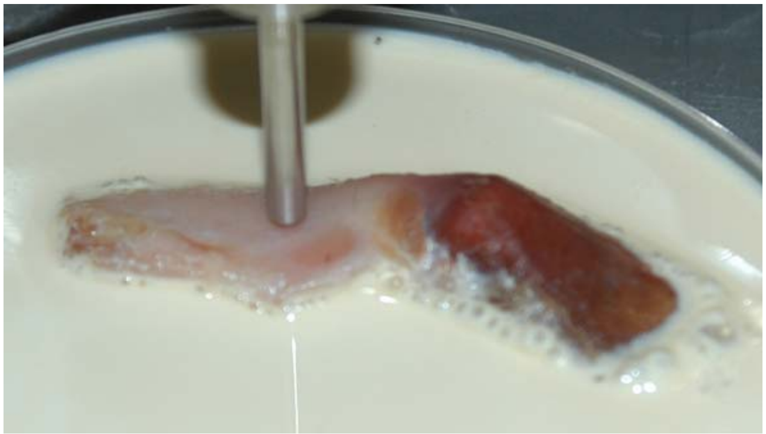

Figure 5: Costal Cartilage Specimen potted in Fast Cast resin.

Indentation Tests

A custom, displacement-controlled indentation instrument was assembled (Figure 6). The driving mechanism was a high precision vertical linear stage (Newport IMS-V100) driven by a Newport XPS C-4 Controller. This provided a driving force of up to 500 N and 0.1µm displacement resolution. A custom LabVIEW virtual instrument (vi) was written to collect data at 100Hz from the load cell (force) and the linear encoder on the stage (displacement). Also, vi's were used to control the motion of the stage.

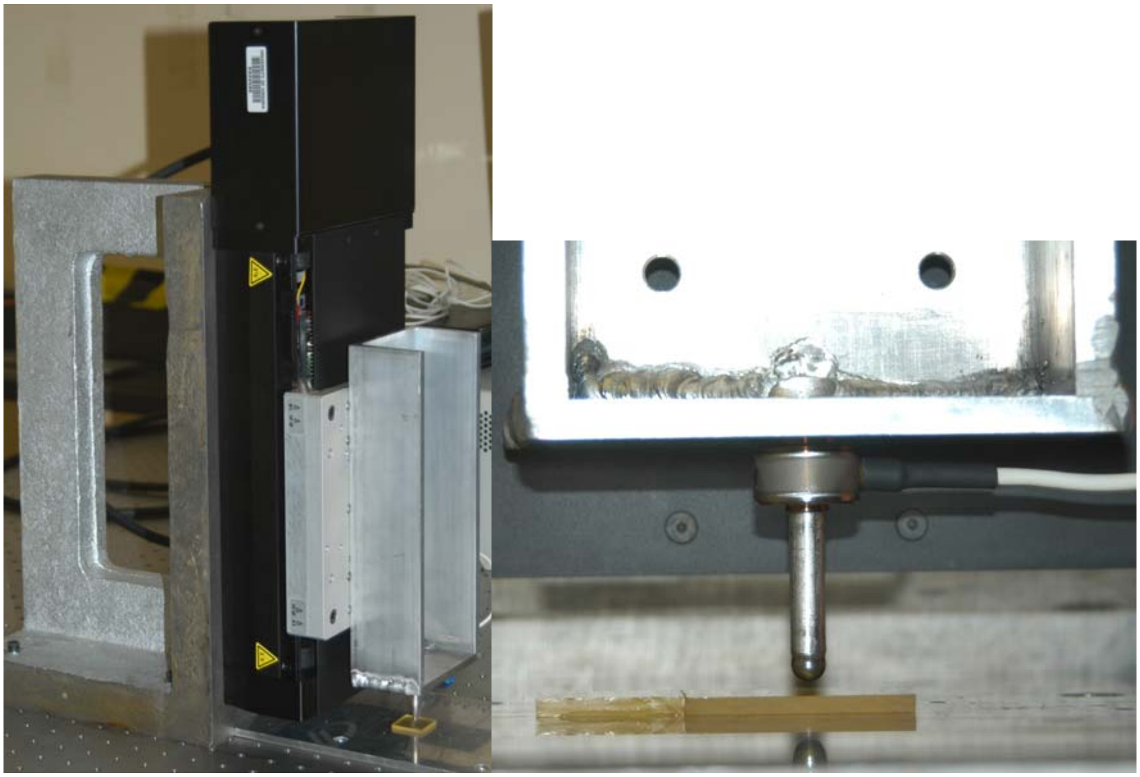

Figure 6: Indentation System (Left). Load cell mounted inline between the linear actuator and the shaft of a 6.35 mm diameter spherical indentation tip (Right).

These were stress relaxation tests in which the spherical tip was given a prescribed displacement into the specimen with a hold time of 120 seconds (Figure 7). The majority of the indentation tests had an indentation depth of $h_{max} = 0.300$ mm, however, some tests were performed at $h_{max} = 0.250$ mm. A smaller indentation depth was used in some cases because the specimen exhibited some bone fracture at the higher depth. These downward displacements are relative to the initial contact point between the indenter tip and the specimen surface. The contact point was determined prior to each test by lowering the probe until the detection of a small preload (0.05 N).

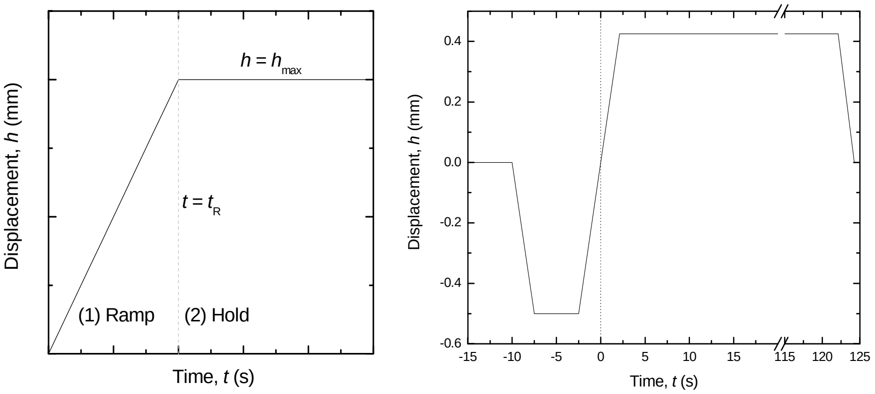

Figure 7: Indentation loading scheme for ramp-hold relaxation tests. (1) Ramp to peak displacement, h_{max}, at displacement rate k given by $k = h_{max} / t_R$ where t_R is the rise time, the time to peak displacement. (2) Peak displacement level, h_{max}, for a holding time of 120 seconds.

These indentation tests were performed on the surface of the specimen starting on the proximal end of the costal cartilage. These tests were performed about 0.5 cm apart moving distally across the costal chondral junction (CCJ) to the rib bone.

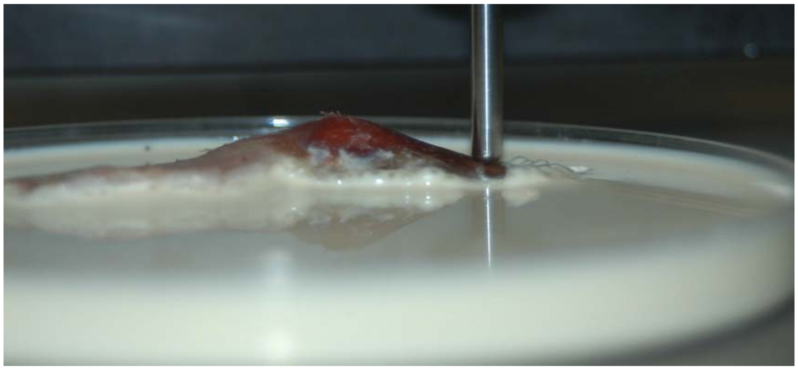

Figure 8: Surface indentation of the costal cartilage.

Analytical Modeling

Since the depth of indentation is less than 10% of the specimen thickness, the effects of the underlying material beneath the specimen can be neglected (Oliver and Pharr, 1992). Also, because there is no closed form analytical solution for displacement controlled spherical indentation with a ramp hold input (Sakai, 2002), an analytical modeling technique has been developed and is outlined in detail in Mattice et al. (2006). In summary, using the viscoelastic correspondence (Lee and Radok, 1960) with the Hertzian contact solution for a sphere (Johnson, 1985) the relaxation response can be expressed as

$$P(t) = \frac{8\sqrt{R}}{3} h_0{}^{3/2} [2G(t)] \qquad (1)$$

where $P(t)$ is the measured load, R is the radius of the spherical tip, h_0 is the indentation depth, and $G(t)$ is the shear relaxation modulus. Equation 1 describes the force relaxation response for an ideal step in displacement, which is impossible to achieve in experimentation. Thus, the Mattice et al. method assumes a step input for the displacement, and takes into account this non-zero ramp time in the displacement with a Ramp Correction Factor (RCF).

Based on pilot data, a three time constant Maxwell model was chosen, with a relaxation function,

$$G(t) = C_0 + C_1 \exp(-t/\tau_1) + C_2 \exp(-t/\tau_2) + C_3 \exp(-t/\tau_3) \qquad (2)$$

The force relaxation portion of the acquired data was fit to

$$P(t) = B_0 + B_1 \exp(-t/\tau_1) + B_2 \exp(-t/\tau_2) + B_3 \exp(-t/\tau_3) \qquad (3)$$

Using the Matlab™ curve fitting toolbox (Version 1.1.6, Matlab Version 7.3), the coefficients were obtained and used to calculate the shear relaxation modulus parameters in Equation 2 using

$$C_0 = \frac{B_0}{h_{\max}^{3/2}(8\sqrt{R}/3)} \qquad (4)$$

$$C_k = \frac{B_k}{(RCF_k)h_{\max}^{3/2}(8\sqrt{R}/3)}, \quad k = 1,2,3 \qquad (5)$$

where

$$RCF_k = \frac{\tau_k}{t_R}\left[\exp\left({t_R}/{\tau_k}\right) - 1\right], \quad k = 1,2,3 \tag{6}$$

and *RCF* is the "ramp correction factor," the difference between the observed values for analysis assuming ramp loading vs the step loading assumption (Oyen, 2005).

From the obtained relaxation moduli, the instantaneous shear modulus (G_0) and long time (G_∞) shear modulus values can be computed:

$$\begin{aligned} G_0 &= G(0) = \frac{C_0 + C_1 + C_2}{2} \\ G_\infty &= G(\infty) = \frac{C_0}{2} \end{aligned} \tag{7}$$

From these values, the instantaneous and long-time elastic modulus values (E_0 and E_∞) can be computed, recalling that for an incompressible solid $E = 3G$.

RESULTS

Cross Sectional indentation of localized calcification regions resulted in different responses not only in the stiffness, but also in the amount of relaxation (Figure 10). These indentations correspond to locations shown in **Figure 9**.

Figure 9: Costal Cartilage Section with white calcification regions.

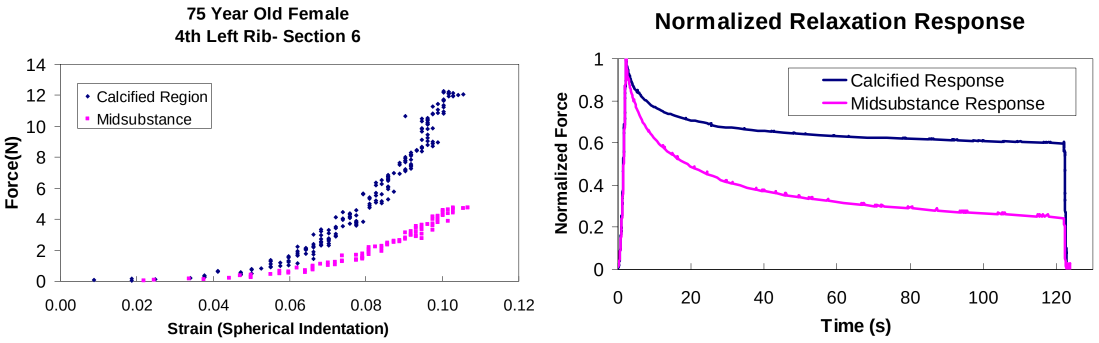

Figure 10: Force-Strain response for calcified region and cartilage midsubstance (Left). Normalized relaxation responses (Right).

Exterior surface indentations were performed along the costal cartilage across the costal chondral junction and onto the rib bone. These tests show an increasing modulus value in addition to a jump in the modulus ratio (E_∞ / E_0 , the relaxed modulus divided by the instantaneous modulus). The results from the indentations performed along exterior surface of costal cartilage moving towards the rib are in **Figure 11**.

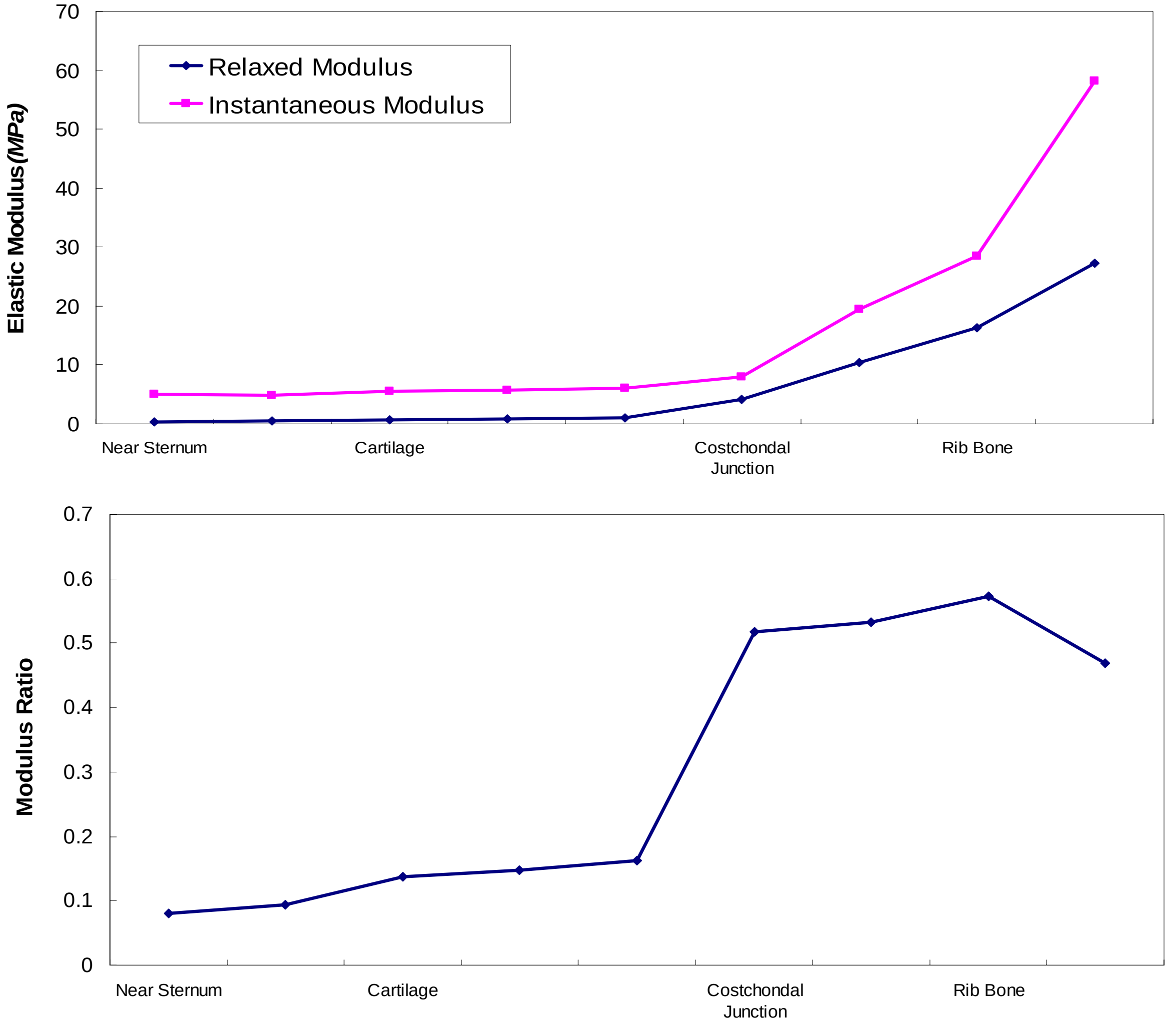

Figure 11: Plot of modulus values (top) and modulus ratio (bottom) as a function of the location along the costal cartilage and rib bone specimen.

Also, microCT analysis found that there was significant infiltration of the rib bone into the costal cartilage midsubstance.

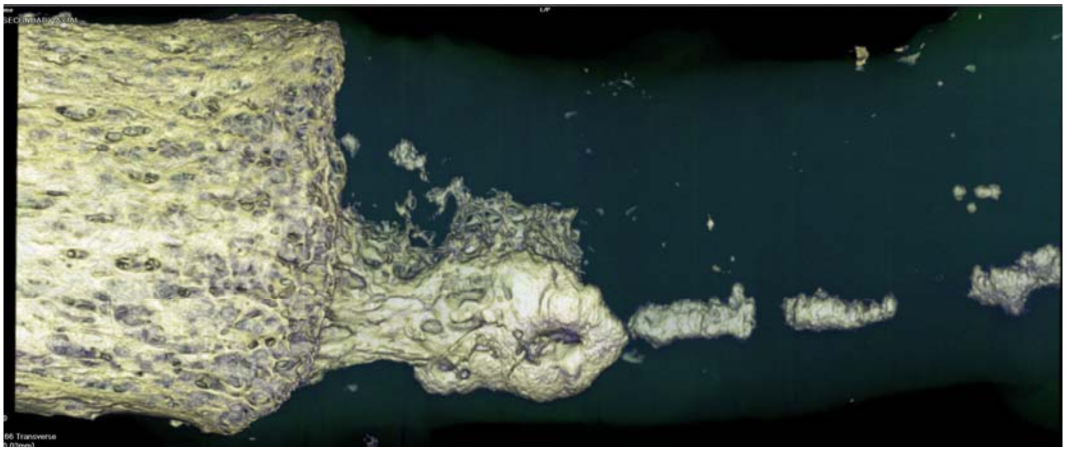

Figure 12: MicroCT rendering of bone infiltration into the costal cartilage. The bone extends from the costal chondral junction area of the rib bone (left) and enters the cartilage midsubstance.

CONCLUSIONS

Major differences in the modulus values between the bone infiltration regions and cartilage were observed. There was significant infiltration of the rib bone into the cartilage midsubstance. This rib bone infiltration of the cartilage would definitely have an effect on the overall mechanical response of the rib cage. Further investigation is needed to fully characterize the properties of this bone infiltration. Knowing more about these calcification regions, finite element models of the thorax can be improved to take into account this bone infiltration.

ACKNOWLEDGEMENTS

Special thanks to Dr. Ed Botchwey from the UVA department of Biomedical Engineering for allowing the use of the microCT scanner.

REFERENCES

CHENG, L., XIA, X., SCRIVEN, L. E., and GERBERICH W. W. (2005). Spherical-tip indentation of viscoelastic material. Mechanics of Materials 37, 213-226.

GUPTA, H. S., SCHRATTER, S., TESCH, W., et al. (2005). Two Different correlations between nanoindentation modulus and mineral content in the bone-cartilage interface. *J Structural Biology* 149:138-148.

JOHNSON, K. L. (1985). Contact Mechanics. UK: Cambridge University Press.

KENT, R., LESSLEY, D. and SHERWOOD, C. (2004). Thoracic response corridors for diagonal belt, distributed, four-point belt, and hub loading. Stapp Car Crash Journal 48:495-519.

LAIB, A. and RUEGSEGGER, P. (1999). Comparison of structure extraction methods for in vivo trabecular bone measurements. *Computerized Medical Imaging and Graphics* 23,69-74.

LAU, A. G., OYEN, M. L., and KENT, R. W. (2006). Indentation Stiffness of Aging Human Costal Cartilage. *Acta Biomaterialia*. Submitted.

LEE, E. H. and RADOK, J. R. M. (1960). Contact problem for viscoelastic bodies. Journal of Applied Mechanics 27, 438-44 .

MATTICE, J. M., LAU, A. G., OYEN, M. L., and KENT, R. W. (2006). Spherical Indentation Load-Relaxation of Soft Biological Tissues. Journal of Materials Research 2006, 8:2003-10.

MOW V. C, GU W. Y., and CHEN, F. H. (2005). Structure and function of articular cartilage and meniscus. Basic Orthopaedic Biomechanics and Mechanobiology, Chapter 5, third edition, Mow VC and Huiskes R, eds. Philadelphia: Lippincott, Williams and Wilkins.

OYEN, M. L. (2005). Spherical Indentation Creep Following Ramp Loading. J. Mater. Res. 2005; 20(8):2094-2100.

OLIVER, W. C. and PHARR, G. M. (1992). Improved technique for determining hardness and elastic modulus using load and displacement sensing indentation experiments. J Mater Res 1992, 7(6):1564-83.

PATTIMORE, D., THOMAS, P., and DAVE, S. (1992). Torso injury patterns and mechanisms in car crashes: an additional diagnostic tool. Injury: The British Journal of Accident Surgery 23, 123-126.

REJTAROVA, O., SLIZOVA, D., SMORANC, P., REJTAR, P., and BUKAC, J. (2004). Costal cartilages - a clue for determination of sex. Biomed Pap Med Fac Univ Palacky Olomouc Czech Repub. 148, 241-3.

ROY, R., KOHLES, S. S., ZAPOROJAN, V., PERETTI, G. M., RANDOLPH, M. A., XU, J., and BONASSAR, L. J. (2004). Analysis of bending behavior of native and engineered auricular and costal cartilage. J Biomed Mater Res A. 68, 597-602.

SAKAI, M. (2002). Time-dependent Viscoelastic Relation Between Load and Penetration for an Axisymmetric Indenter. Philosophical Magazine. Vol. 82, No 10: 1841-1849.

STITZEL, J. D., CORMIER, J. M., BARRETTA, J. T., KENNEDY, E. A., SMITH, E. P., RATH, A. L., DUMA, S. M., and MATSUOKA, F. (2003). Defining regional variation in the material properties of human rib cortical bone and its effect on fracture prediction. Stapp Car Crash Journal 47:243-65.

TEAL, C., ROMANIUK, C., and MULLEY, G. (1989). Calcification on Chest Radiographs: The Association with Age. Age and Ageing 18:333-336.

DISCUSSION

PAPER: **Material Characterization of the Costal Chondral Junction**

PRESENTER: ***Anthony Lau, University of Virginia Center for Applied Biomechanics***

QUESTION: *Erik Takhounts, Chair*
Before Guy comes in, I will ask you a question.

ANSWER: Sure.

Q: The indentation test is basically a compression test?

A: Yes. It's primarily in compression.

Q: Let me ask a question. But, you were talking about the sheer modulus and you were talking about the elastic modulus. How do you determine--?

A: It's actually outlined more in detail in the paper. I can give you—But basically, make an assumption that the costal cartilage is, the Poissant ratio is, in compressibles, is .5. And then from there, we can derive -- I think it's like 1 over 2 meters.

Q: Right.

A: Okay, from sheer modulus to elastic modulus. We use viscoelastic correspondence, too. I could get you that paper.

Q: Yeah. I know that paper. I'm just wondering what kind of assumptions, you know. Okay. Now it's clear. Are you gonna try to do the quasi-, quasi-linear material model?

A: Well, our preliminary tests found that we don't really, at these strain levels, have a quasi-linear model yet. We're still at fairly low restraint levels. So we performed indentation tests at various depths and there's no drastic changes at these levels yet.

Q: Okay. Thanks.

Q: *Guy Nusholtz, Daimler Chrysler*
Have you done any evaluation to find out what the magnitude of the problem is? You have a discontinuity in the model, but what affect does that have on the response of the model?

A: We have not done any finite element modeling yet. These are fairly recent findings and I mean, again, we can use these—I mean, the microCTs provide us with nice geometries. I guess we could always say: If you have basically bone surrounding the cartilage, you're changing the actual the location, you know. If you assume that you have soft tissue and then hard tissue, you're actually changing the location of the transition and also changing the material properties at those regions.

Q: Yeah, but what's the magnitude of a problem? Let's say you have a belt load or you have an impactor load, and you have a case where you smear it—You smear the properties across a wider range and you have a discontinuity: What's the difference in response?

A: Oh, we have not looked at that yet. We have some finite element models that when we changed the properties of the costal cartilage itself, it just changed the chest concentration in the ribs, and I can show you those diagrams.

Q: Okay. So that would be some indication of what the problem is. But before you—I mean, you're going into a lot of detail without first scoping out what the magnitude of the problem is and to what level you really need to collect, to correct it. So, it would seem that it would help you to focus where your project going if you first sort of figure out: What is the problem with having the discontinuity and how sensitive is it to small changes?

A: Okay. We can take a look at that.

Q: Thank you.

Q: *Stephen Duma, Virginia Tech*
Nice work. Having done some cartilage indentation, I can appreciate the complexity. What was your total deflection you're indentating? What kind of range are--?

A: Oh. We're at .425 micro millimeters, so it's still in the micro range.

Q: Experimentally, a couple questions: One is, how do you know where your zero point is when you touch the cartilage, and the second question is, how do you know you're perpendicular or at that low level, there's not some geometric irregularity in the sample or something?

A: Yeah. Well, again, in homogeneous, we try to prepare the cartilage specimens as flat as possible and along with—As one benefit of actually using spherical, we're not as sensitive to the alignments of the actual indentation code as opposed to, like, a flat indenture where you have to prepare for any surface variation because of discrepancies in the data. As for the contact point: We lower it down to where the load cell reaches 0.05 newtons. Basically, just touching it. And, we can also, kind of, by backing away from the cartilage, before going back in, we can also go back and look at the data and say, you know, "Hey. We know where the force starts to pick up," and we can determine the contact point there because we also record actually the depth data of location.

Q: Right, right. Well, that sounds good. It's impressive work, like I said. I mean, 0.50 newtons and getting that right, I think using the sphere's the appropriate way to do it well. So, congratulations. Thanks.

Q: *Erik Takhounts, Chair*
Let me ask you one more question. You assume about this transition, but you also assume that all the transitional material properties happen actually on the surface where you can pick up with indentation methods. How about if the transition actually is in the cartilage?

A: Well, that's why we did the cross-sectional indentations because that's why we're doing both surfaces. Because, yes, on the surface, we're kind of getting a macro scale. You know, we can go back to this picture here. This is just a two-dimension view, but we can see that there's a rib bone protruding in. So if we do surface indentations, those two—the infiltrating rib bone—will contribute. Then by additionally doing cross-sectional, we can say, "Hey. We can look at the cartilage inside and try to test the rib bone as it transitions."